Nuclear-Charge Distribution in Low-Energy Fission*

A. C. Wahl, R. L. Ferguson,† D. R. Nethaway,‡ D. E. Troutner,§ and K. Wolfsberg‖

Department of Chemistry, Washington University, St. Louis, Missouri

New information concerning half-lives and fractional independent and fractional cumulative yields of fission products has been obtained from experiments in which adjacent elements in fission-product chains were rapidly separated.

Fractional cumulative yields that have been determined for the thermal-neutron fission of U^{235} are: Kr^{93}, $0.075_{-0.002}^{+0.010}$; Kr^{94}, $0.015_{-0.002}^{+0.005}$; Kr^{95}, $(1.1_{-0.1}^{+0.3}) \times 10^{-3}$; Kr^{97}, $<10^{-5}$; Xe^{137}, 0.978 ± 0.003; Xe^{138}, 0.956 ± 0.003. Fractional cumulative yields determined for the spontaneous fission of Cf^{252} are: Xe^{139}, 0.67 ± 0.01; Xe^{140}, 0.45 ± 0.01; Xe^{141}, 0.172 ± 0.005; Xe^{144}, <0.007.

Fractional independent yields determined for the thermal-neutron fission of U^{235} are: Sr^{91}, 0.07 ± 0.05; Nb^{95m}, $<4\times10^{-5}$; Nb^{96}, $(1.0\pm0.2)\times10^{-4}$; Nb^{97}, $(1.7\pm0.8)\times10^{-3}$; Cs^{136}, $(1.10\pm0.15)\times10^{-3}$; Ba^{139}, $0.012_{-0.003}^{+0.005}$; Ba^{140}, 0.066 ± 0.026; Ba^{141}, 0.27 ± 0.08; La^{141}, 0.004 ± 0.002; La^{142}, 0.019 ± 0.005; Ce^{143}, $(4.4\pm3.0)\times10^{-3}$. Fractional independent yields determined for the thermal-neutron fission of U^{233} are: Nb^{95m}, $<3\times10^{-4}$; Nb^{96}, $(1.3\pm0.2)\times10^{-3}$; Nb^{97}, 0.011 ± 0.004. Fractional independent yields determined for the thermal-neutron fission of Pu^{239} are: Nb^{95m}, $<3\times10^{-4}$; Nb^{96}, $(7.7\pm1.0)\times10^{-4}$; Nb^{97}, 0.015 ± 0.004. The fractional independent yield of Cs^{136} from spontaneous fission of Cf^{252} is <0.01.

The above data together with other published data give direct information about the distribution of nuclear charge among fission products with mass numbers 91, 139, 140, 141, 142, and 143 from thermal-neutron fission of U^{235}. The variation of fractional yield with Z for constant A can be represented in cumulative form by the area under a Gaussian curve from $-\infty$ to $Z+\frac{1}{2}$. The standard deviation of the curve which best represents the data for the six mass numbers is $\sigma=0.62\pm0.06$.

The variation with A of Z_P, the value of Z at the maximum in a charge distribution curve, is discussed, and a new empirical Z_P function is derived on the assumption that the Gaussian curve is applicable to all mass numbers. The function and curve correlate quite well the available fractional yield data for low-energy fission processes.

There are indications from the analysis of charge dispersion, and from some other observed fission phenomena, that primary low-energy fission products with Z less than 50 and greater than the complementary charge (>42 for $_{92}U$ fission) may be formed in very low yield. It is suggested that observed fission products with atomic numbers in this range may be formed predominantly by beta decay processes starting from products complementary to $_{50}Sn$ ($_{42}Mo$ for $_{92}U$ fission) or from products of lower Z.

During the course of this work, fission yields of 51-min Nb^{98} from thermal-neutron fission of U^{235}, U^{233}, and Pu^{239} were determined to be $(0.064\pm0.012)\%$, $(0.20\pm0.03)\%$, and $(0.20\pm0.03)\%$, respectively.

New half-life values determined are: Rb^{91}, 72 ± 8 sec; Rb^{92}, <11 sec; Nb^{98}, 51 ± 3 min; Cs^{141}, 25 ± 3 sec; Cs^{142}, <8 sec; Ba^{143}, 12 ± 2 sec. Kr^{97} and a reported 14-min isomer of Rb^{91} were not found among the fission products; we believe that our data refute the published evidence for their existence.

INTRODUCTION

ALTHOUGH the distributions of mass among products of many low-energy fission processes are known quite well,[1] relatively little is known about the distributions of nuclear charge. Mass distributions are obtained from measurements of cumulative yields of late members of fission-product chains after beta decay of early short-lived members is substantially complete. Charge distributions are obtained from primary yields of individual fission products, most of which are very short lived and/or are formed mainly by beta decay of short-lived precursors. Thus primary yields for most fission products are difficult to measure, and consequently relatively few have been measured.

Some understanding of nuclear charge distribution in fission has been gained from the formulation of postulates[2–9] and comparison of predicted primary yields with the few measured ones. The primary or independent yields are usually expressed as fractional yields (fractions of total chain yields). Fractional cumulative yields that are significantly less than unity are also useful. It has been assumed for the yield predictions that the same smooth and symmetrical charge distribution curve[2,4] (fractional independent yield vs Z) is appropriate for all mass numbers, and estimates have been made for each mass number of Z_P, the position on the Z axis of the maximum in the curve. The assumption that a single charge distribution curve is appropriate for all mass numbers has been necessary because not more than one fractional yield has been known for any one mass number.

In this paper some methods of rapidly separating

[1] S. Katcoff, Nucleonics 18, No. 11, 201 (1960).

[2] L. E. Glendenin, C. D. Coryell, and R. R. Edwards, *Radiochemical Studies: The Fission Products*, edited by C. D. Coryell and N. Sugarman (McGraw-Hill Book Company, Inc., New York, 1951), National Nuclear Energy Series, Plutonium Project Record, Vol. 9, Div. IV, p. 489.

[3] A. C. Pappas, Massachusetts Institute of Technology Report No. 63 (AECU-2806), 1953 (unpublished).

[4] A. C. Pappas, *Proceedings of the International Conference on the Peaceful Uses of Atomic Energy, Geneva, 1955* (United Nations, Geneva, 1956), Vol. 7, pp. 19–26.

[5] E. P. Steinberg and L. E. Glendenin, *Proceedings of the International Conference on the Peaceful Uses of Atomic Energy, Geneva, 1955* (United Nations, Geneva, 1956), Vol. 7, pp. 3–14.

[6] T. J. Kennett and H. G. Thode, Phys. Rev. 103, 323 (1956).

[7] W. E. Grummitt and G. M. Milton, Chalk River Laboratory Report CRC-694 (AECL-453), 1958 (unpublished).

[8] A. C. Wahl, J. Inorg. & Nuclear Chem. 6, 263 (1958).

[9] C. D. Coryell, M. Kaplan, and R. D. Fink, Can. J. Chem. 39, 646 (1961).

adjacent members of fission-product chains are described, and new half-lives and fractional cumulative and independent yields that have been measured are reported. Fractional yields for two or more members of each of six chains give direct information about the shapes of the charge distribution curves for these chains from thermal-neutron fission of U^{235}. On the assumption that the best single curve for these chains is applicable to other chains and to other low energy fission processes, a new empirical Z_P function is derived.

EXPERIMENTAL

Irradiations

Most irradiations with thermal neutrons were made at the Washington University cyclotron in a paraffin block behind a beryllium target that was bombarded with 10-Mev deuterons. Salts or solutions of uranium enriched to 20% in U^{235} were irradiated. The thermal-neutron flux was about 4×10^8 cm^{-2} sec^{-1} at the position in the paraffin block where pneumatic rabbit cartridges were irradiated. Farther back in the block where other containers were irradiated for emanation experiments the flux was about 7×10^7 cm^{-2} sec^{-1}. The ratio of fissions produced by thermal neutrons to those produced by higher energy neutrons was about 70 as measured from the radioactivities of Zr^{97}, Ba^{139}, and Ba^{140} produced in uranium irradiated with and without 0.060 in. of cadmium wrapping.

Some irradiations were carried out in the 4W column of the Los Alamos homogeneous reactor, where thermal-neutron fluxes were (1 to 6)$\times 10^{11}$ cm^{-2} sec^{-1}. For yields of niobium nuclides, thin oxide films of U^{233}, U^{235}, and Pu^{239} on platinum were covered with aluminum catcher foils and irradiated; the aluminum foils were analyzed radiochemically. For yields of inert-gas nuclides, irradiation of uranyl stearate in an evacuated container was limited to about 1.5×10^{12} fissions so that the small amount of radiation decomposition produced, resulting in about 5 mm of Hg pressure, would not affect the emanating power. (One irradiation giving 5×10^{13} fissions resulted in considerable decomposition, a pressure of about 100 mm of Hg, and some loss of emanating power.)

A source of Cf^{252} mounted on platinum was obtained from the Argonne National Laboratory. Recoiling fragments from spontaneous fission were caught in barium or lanthanum stearate in an evacuated irradiation container. The relative strength of the source was followed during the course of the experiments. Aluminum catcher foils were exposed to the source for the arbitrary but definite time of 16.00 hr, and the beta activity of the fission products in the foils was then measured. The absolute strength of the source was determined by fission counting after the conclusion of the experiments. The intensity during the experiments was about 8×10^4 fissions per minute.

Procedure

In all experiments the radioactivities of two samples from the same irradiation were compared. For independent-yield measurements an irradiated sample was divided into two portions. In one, a fission product was chemically separated from its precursors as soon as possible after the irradiation in order to maximize the fraction of the product formed independently. In the second, the separation was made after extensive decay of the precursors. In the emanation experiments for the determination of krypton and xenon cumulative yields, the inert gases diffused from the stearate salt during the irradiation and deposited their descendants on filter paper which lined the walls of the container. The samples compared came from the filter paper (fission products with inert gas precursors) and from the stearate salt (fission products without inert gas precursors).

After the initial separations, which are described in the Appendix, the element of interest was purified, usually by modifications[10-18] of standard radiochemical procedures [strontium,[14] yttrium (a new method),[12] zirconium,[15] niobium,[16-18] cesium,[19] barium,[20] lanthanum,[13,21] cerium[22,23]]. The activities of the fission product from each portion were determined in samples mounted in the same way, with the same counter, and in the same geometry, and so were directly comparable without counting efficiency corrections.

[10] R. L. Ferguson, Ph.D. thesis, Washington University, 1959; University Microfilms (Ann Arbor, Mich.), L. C. Card No. Mic. 59-1742.

[11] D. E. Troutner, Ph.D. thesis, Washington University, 1959; University Microfilms (Ann Arbor, Mich.), L. C. Card No. Mic. 59-6945.

[12] K. Wolfsberg, Ph.D. thesis, Washington University, 1959; University Microfilms (Ann Arbor, Mich.), L. C. Card No. Mic. 59-6946.

[13] D. R. Nethaway, Ph.D. thesis, Washington University, 1959; University Microfilms (Ann Arbor, Mich.), L. C. Card No. Mic. 60-63.

[14] L. E. Glendenin, *Radiochemical Studies: The Fission Products*, edited by C. D. Coryell and N. Sugarman (McGraw-Hill Book Company, Inc., New York, 1951), National Nuclear Energy Series, Plutonium Project Record, Vol. 9, Div. IV, p. 1460.

[15] C. W. Stanley and G. P. Ford, Los Alamos Scientific Laboratory Report LA-1721, 1954 (unpublished), p. 109.

[16] J. S. Gilmore, Los Alamos Scientific Laboratory Report LA-1721, 1954 (unpublished), p. 115.

[17] L. E. Glendenin, *Radiochemical Studies: The Fission Products*, edited by C. D. Coryell and N. Sugarman (McGraw-Hill Book Company, Inc., New York, 1951), National Nuclear Energy Series, Plutonium Project Record, Vol. 9, Div. IV, p. 1523.

[18] H. G. Hicks and R. S. Gilbert, Anal. Chem. 26, 1205 (1954).

[19] H. B. Evans, *Radiochemical Studies: The Fission Products*, edited by C. D. Coryell and N. Sugarman (McGraw-Hill Book Company, Inc., New York, 1951), National Nuclear Energy Series, Plutonium Project Record, Vol. 9, Div. IV, p. 1646.

[20] L. E. Glendenin, *Radiochemical Studies: The Fission Products*, edited by C. D. Coryell and N. Sugarman (McGraw-Hill Book Company, Inc., New York, 1951), National Nuclear Energy Series, Plutonium Project Record, Vol. 9, Div. IV, p. 1657.

[21] K. Wolfsberg, D. R. Nethaway, H. P. Malan, and A. C. Wahl, J. Inorg. & Nuclear Chem. 12, 201 (1960).

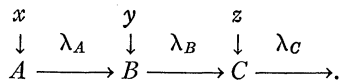[22] L. E. Glendenin, K. F. Flynn, R. F. Buchanan, and E. P. Steinberg, Anal. Chem. 27, 59 (1955).

[23] H. G. Hicks, University of California Radiation Laboratory Report UCRL-4377, 1954 (unpublished), p. 12.

For determination of the yields of Nb^{96}, Nb^{98}, and Cs^{136}, radioactivities were measured with beta proportional counters, some of which (those at Los Alamos) had been calibrated absolutely by Bayhurst and Prestwood.[24] The other counters were similar to these in sample-counter geometry and in absorber thickness and so were assumed to have the same counting efficiency for samples mounted in the same way. The Nb^{96}, and Nb^{98} radioactivities were compared to that of Zr^{97}, which has fission yields[1,11] of 6.0%, 4.8%, and 5.5% for thermal-neutron fission of U^{235}, U^{233}, and Pu^{239}, respectively. The radioactivity of Cs^{136} was compared with that of Ce^{144}, which has a yield[5] of 5.7% from thermal-neutron fission of U^{235}.

Definitions and Calculations

Consider the fission-product decay chain:

$$\begin{array}{ccccc} x & & y & & z \\ \downarrow & \lambda_A & \downarrow & \lambda_B & \downarrow \quad \lambda_C \\ A & \longrightarrow & B & \longrightarrow & C \longrightarrow . \end{array}$$

Define:

$x=$fractional cumulative yield of A, based on the cumulative yield of C.

y, $z=$fractional independent yields of B and C, respectively, based on the cumulative yield of C.

$T=$duration of irradiation producing fissions at a constant rate.

t, $t'=$time intervals between the end of an irradiation and the separation of adjacent chain members for the two samples from the same irradiation.

$\tau=T/2+t$; $\tau'=T/2+t'$.

$Q=$ratio of activity of C separated after t to activity of C separated after a longer time t', corrected for chemical yield, to the same number of fissions, and for decay to the same time.

$Q^*=Q\exp[\lambda_C(t'-t)]=1/M$ (M as is defined in reference 25).

$R=$fraction of B remaining with nuclide C after initial rapid separation of C from B.

$\Delta t=$time interval between initial rapid separation of B from C and subsequent separation (assumed to be complete).

$G=$ratio of activity of B, C or later chain member from irradiation-container liner to the activity of the same chain member from the stearate salt, corrected for chemical yield, for incomplete recovery of the stearate salt, and for decay to the same time.

$f=$fraction of the total empty space in the irradiation container that is between the grains of stearate salt.

$\epsilon=$efficiency of collection of active deposit on the irradiation container liner.

$E=$fraction of inert-gas nuclide formed in the stearate salt that escapes under the conditions of the irradiation (emanating power).

$$J=[1-\exp(-\lambda_A T)]\exp(-\lambda_A t),$$
$$K=[1-\exp(-\lambda_B T)]\exp(-\lambda_B t).$$
$$L=[1-\exp(-\lambda_C T)]\exp(-\lambda_C t),$$
$$J'=[1-\exp(-\lambda_A T)]\exp(-\lambda_A t'), \quad \text{etc.}$$

$$a=\frac{\lambda_B\lambda_C}{(\lambda_B-\lambda_A)(\lambda_C-\lambda_A)}, \quad b=\frac{\lambda_A\lambda_C}{(\lambda_A-\lambda_B)(\lambda_C-\lambda_B)},$$

$$c=\frac{\lambda_A\lambda_B}{(\lambda_A-\lambda_C)(\lambda_B-\lambda_C)}.$$

$$\bar{b}=\frac{\lambda_C}{\lambda_C-\lambda_B}, \quad \bar{c}=\frac{\lambda_B}{\lambda_B-\lambda_C}, \quad d=\frac{\lambda_A-\lambda_C}{\lambda_B-\lambda_C}.$$

From the standard equations of radioactive transformation[26] the following equation has been derived.

$$z=\frac{a(1-y)\Gamma+[b(1-y)+\bar{b}y]\Lambda+[c(1-y)+\bar{c}y](Q-1)L}{a\Gamma+b\Lambda+(c-1)(Q-1)L},$$
$$\tag{1}$$

where

$$\Gamma=Q^*J'-J+JdR\{1-\exp[(\lambda_C-\lambda_B)\Delta t]\},$$
and
$$\Lambda=Q^*K'-K+KR\{1-\exp[(\lambda_C-\lambda_B)\Delta t]\}.$$

The evaluation of this equation was programmed for the IBM 704 computer; calculations were made at the Los Alamos Scientific Laboratory.

For $R=0$ or $\Delta t=0$ and for t' very long compared to the periods of A and B ($J'=0$ and $K'=0$), Eq. (2) is applicable.

$$z=\frac{axJ+[bx+\bar{b}(1-x)]K+[cx+(1-\bar{b})(1-x)]L(1-Q)}{\bar{b}[K-L(1-Q)]}.$$
$$\tag{2}$$

For $\lambda_A\gg\lambda_C$ and $\lambda_B\gg\lambda_C$ and with the approximations that

$$[1-\exp(-\lambda_B T)]=\lambda_B T[\exp(-\lambda_B T/2)]$$
and
$$[1-\exp(-\lambda_C T)]=\lambda_C T[\exp(-\lambda_C T/2)],$$

Eq. (2) reduces to Eq. (3), which is useful when neither λ_B nor z is known.

$$\ln[(1-Q)\exp(-\lambda_C\tau)+F]=\ln(H)-\lambda_B\tau, \tag{3}$$
where
$$F=\frac{x\lambda_B[1-\exp(-\lambda_A T)]\exp(-\lambda_A t)}{\lambda_A(\lambda_A-\lambda_B)T}. \tag{3a}$$

[24] B. P. Bayhurst and R. J. Prestwood, Nucleonics 17, No. 3, 82, (1959).

[25] A. C. Wahl, Phys. Rev. 99, 730 (1955).

[26] See, for example, W. Rubinson, J. Chem. Phys. 17, 542 (1949).

and

$$H = 1 - z + x\lambda_B/(\lambda_A - \lambda_B). \tag{3b}$$

When F is small compared to $(1-Q) \exp(-\lambda_C\tau)$, as it is when C is Sr^{91}, Sr^{92}, Ba^{141}, Ba^{142}, or Ba^{143} from $U^{235}(n_{th},F)$, a plot of $\log[(1-Q) \exp(-\lambda_C\tau)]$ vs τ results in a straight line of slope $\lambda_B/2.303$ and an intercept of $\log(H)$. From this value of λ_B, F may be calculated and a second plot made, as is illustrated in Fig. 1.

For the decay chains treated by the above method, limitations on the validity of the approximations made in the derivation of Eq. (3) affect only the terms F and H. The corrections for F are small ($<3\%$) and, since F itself is small, can be neglected. Corrections for H are negligible ($<0.2\%$) for the $A = 91$ and 141 chains and are 13% for the $A = 143$ chain. Therefore, the slopes of the plots suggested above give reliable values of λ_B, and the intercepts give $\log(H)$ for $A = 91$ and 141 and $\log(1.13H)$ for $A = 143$.

For a two membered chain ($J = 0$, $J' = 0$, $\lambda_A \gg \lambda_C$, $\lambda_A \gg \lambda_B$) in which $\lambda_C > \lambda_B$ and $t' \gg 1/\lambda_C$ ($Q = 0$),

$$z = 1 - L/\bar{b}(Q^*K' - K + L). \tag{4}$$

For the emanation experiments, it is assumed that the inert gas that escapes from the stearate salt is uniformly distributed in the free space within the irradiation container.

When the irradiation container is opened (at time t) before all of an inert gas (B) has decayed, the fractional independent yield of the first decay product (C) is
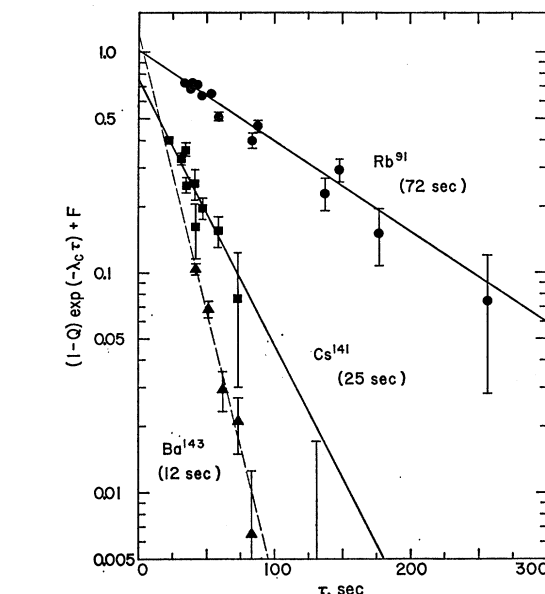

FIG. 1. Half-lives of Rb^{91}, Cs^{141}, and Ba^{143} from timed separations of their daughters. See Eq. (3).

given by

$$z = \frac{a(1-y)J + [b - y(b-\bar{b})]K + [c - y(c-\bar{c})]L}{aJ + bK + L[c + G/\{\epsilon E(1-f) - G(1-E+Ef)\}]}. \tag{5}$$

When an inert gas is allowed to decay essentially completely before the irradiation container is opened,

TABLE I. Fractional cumulative yields.

Fission product	Half-life	Descendant determined	No. of determinations	Average $G \times 100$	Emanating power (E)	% cumulative yield ($w \times 100$)[a]
$U^{235}(n,F)$:						
Kr^{92}	3.0 ± 0.5 sec	Sr^{92}	4	43.5 ± 0.5	>0.95	31.2 ± 0.5[b]
Kr^{93}	2.0 ± 0.5 sec	Y^{93}	8	7.8 ± 0.1	>0.90	$7.5_{-0.2}^{+1.0}$[c]
Kr^{94}	1.4 ± 0.5 sec	Y^{94}	2	1.49 ± 0.17	>0.84	$1.5_{-0.2}^{+0.5}$[c]
Kr^{95}	$1-2$ sec[d]	Zr^{95}	3	0.107 ± 0.005	>0.86	$0.11_{-0.01}^{+0.03}$[c]
Kr^{97}	>0.1 sec[e]	Zr^{97}	2	$(1.9 \pm 0.2) \times 10^{-4}$	>0.22	<0.001[f]
Xe^{137}	3.9 min	Cs^{137}	2	$(2.65 \pm 0.20) \times 10^3$	1.00	97.8 ± 0.3[c]
Xe^{138}	17 min	Cs^{138}	5	$\cdots$	1.00	95.7 ± 0.2[g]
$Cf^{252}(SF)$:						
Xe^{139}	41 sec	Ba^{139}	4	197 ± 4	1.00	67 ± 1
Xe^{140}	16 sec	Ba^{140}	3	79 ± 1	1.00	45 ± 1
Xe^{141}	1.7 sec	Ce^{141}	3	20.3 ± 0.4[h]	>0.98	17.2 ± 0.5
Xe^{144}	1 sec	Ce^{144}	3	<0.65	>0.96	<0.7

[a] The fractional cumulative yield was calculated from Eq. (6) with $\epsilon = 0.98 \pm 0.03$ (see reference 8) and $f = 0.014 \pm 0.002$ for $U^{235}(n,F)$, and $f = 0.005 \pm 0.002$ for $Cf^{252}(SF)$. The error in the positive direction has been increased to make allowance for the possible incomplete emanation, denoted in the preceding column.

[b] Used for calibration; uncorrected for possible incomplete emanation. (See reference 12.)

[c] Data from reference 12.

[d] Half-life consistent with data of Dillard, Adams, Finston, and Turkevich.[28]

[e] Estimated[12] from beta-decay systematics and Cameron's mass formula.[29]

[f] Only an upper limit is meaningful because the small amount of Zr^{97} found on the paper liner may have been due to contamination, or it may have been produced from U or Zr impurities in the paper. However, the small amount of Zr^{97} present can be used to show that the larger amount of Zr^{95} found on the paper was not from these sources.[12]

[g] From the independent yield of Cs^{138}, calculated by Eq. (5). Data for one experiment are: $T = 29$ min, $t = 10.1$ min, $G = 13.1$. The average of the five values of z, calculated on the assumption that $x = y$, is 0.0425 ± 0.0008. Changing to $x = 0$ or to $y = 0$ changes z <0.0001. An uncertainty of ± 1 min in the half-life of Xe^{138} causes an uncertainty of 0.0011 in z. The possible escape of some Xe^{138} from the filter-paper shield or from the aluminum adjacent to the uranyl stearate may have caused the measured z to be low by 0.0005 ± 0.0003.[12]

[h] Measured values of G for two of the experiments have been lowered 2% to correct for Ce^{141} formed in the stearate fraction, after disassembly of the irradiation container, from Cf^{252} that had vaporized during the irradiation, due to local heating by the fission fragments,[30] and had deposited in the stearate salt. In the third experiment an early separation of Ce and Cf eliminated the necessity for the correction. The rate of loss of material by vaporization varied about a factor of two, depending on conditions and on the age of the sample; the average rate was $\approx 10^{-4}$ day^{-1} (approximately 4 atoms vaporized per fission).

TABLE II. Fractional independent yields.

Fission product	No. of determinations	Percent independent yield	
		Average ($z \times 100$)	Selected ($z \times 100$)[a]
$U^{235}(n,F)$:			
Sr^{91}	...	...	7 ± 5[b]
Nb^{95m}	2	<0.004	<0.004[c]
Nb^{96}	2	0.010 ± 0.001	0.010 ± 0.002[d]
Nb^{97}	5	0.17 ± 0.02	0.17 ± 0.08[e]
Cs^{136}	1	...	0.110 ± 0.015[f]
Cs^{138}	2	4.6 ± 0.2[g]	4.4 ± 0.3[g]
Ba^{139}	5	1.2 ± 0.2	$1.2_{-0.3}^{+0.5}$[h]
Ba^{140}	6	6.6 ± 1.3	6.6 ± 2.6[i]
Ba^{141}	...	...	27 ± 8[j]
La^{141}	5	0.36 ± 0.02	0.36 ± 0.17[k]
La^{142}	5	1.9 ± 0.1	1.9 ± 0.5[l]
Ce^{143}	5	0.44 ± 0.07	0.44 ± 0.30[m]
$U^{233}(n,F)$:			
Nb^{95m}	2	<0.03	<0.03[c]
Nb^{96}	2	0.130 ± 0.003	0.13 ± 0.02[d]
Nb^{97}	2	1.1 ± 0.1	1.1 ± 0.4[e]
$Pu^{239}(n,F)$:			
Nb^{95m}	3	<0.03	<0.03[c]
Nb^{96}	3	0.077 ± 0.003	0.077 ± 0.010[d]
Nb^{97}	2	1.5 ± 0.1	1.5 ± 0.4[e]
$Cf^{252}(SF)$:			
Cs^{136}	2	<1.0	<1.0[n]

[a] The errors are estimated to include all known experimental uncertainties, such as those in timing and in half-lives, as well as the standard deviation of the average value.

[b] From the intercept in Fig. 1, $H = 1.020 \pm 0.045$. A 2-sec uncertainty in τ increases the error to ± 0.049. Use of Eq. (3b) with $x = 0.59 \pm 0.01$,[8] $\lambda_A(Kr^{91}) = 0.071$ sec^{-1} (20% uncertainty estimated) and $\lambda_B(Rb^{91}) = 0.0096 \pm 0.0010$ sec^{-1} (see Fig. 1 and the Appendix) gives the independent yield of Sr^{91} shown.[10]

[c] The upper limit is estimated from residual activities (1 to 10 counts/min) with half-lives >23 hr and <35 day in the Nb^{96} samples. The total chain yields for $A = 95$ from thermal-neutron fission of U^{235}, U^{233}, and Pu^{239} are taken to be 6.3%, 6.1%, and 5.1%, respectively.[11]

[d] The error includes an estimated 10% uncertainty in the counting efficiency. A half-life of 23.3 hr is used. The total chain yields for $A = 96$ from thermal-neutron fission of U^{235}, U^{233}, and Pu^{239} are taken to be 6.3%, 5.6%, and 5.4%, respectively.[11] Other reported values of z for Nb^{96} are 0.009%, 0.014% (from compilation in reference 8), and $(0.009 \pm 0.002)\%$[31] for $U^{235}(n_{th},F)$ and $(0.10 \pm 0.02)\%$[31] and $(0.067 \pm 0.010)\%$[31] for $U^{233}(n_{th},F)$ and $Pu^{239}(n_{th},F)$, respectively.

[e] Equation (4) was used in the calculations. Data from one experiment with U^{235} are: $T = 3.5$ min, $t = 3.0$ min, $t' = 1322$ min, $Q^* = 0.152$ giving $z = 1.7 \times 10^{-3}$. Uncertainties in the Nb^{97} and Nb^{98} half-lives, estimated to be ± 1 min and ± 2 min, respectively, caused some uncertainty in the resolution of decay curves, and this caused most of the uncertainty in the value of z.[11]

[f] In an emanation experiment, all of the 12.9-day Cs^{136} formed in fission was found in the uranyl stearate, none on the filter-paper liner.[12] This proves, as has always been assumed, that essentially all Cs^{136} is formed independently and not by beta decay of an unknown isomer of Xe^{136}. The total chain yield for $A = 136$ is taken to be 6.4%.[1] Other reported values of z are 0.9×10^{-3}, 1.0×10^{-3} (from compilation in reference 8), $(0.94 \pm 0.04) \times 10^{-3}$ (from reference 32), and 1.14×10^{-3} (from reference 33).

[g] The average value is from gas sweeping experiments. Equation (1) was used for the calculations, the approximation being made that $x = y$. Data for one experiment are: $T = 1.00$ min, $t = 0.32$ min, $t' = 20.07$ min, $Q = 0.109$ giving $z = 0.048$. If $x = 0$ or $y = 0$, the value of z is changed by 0.0025. An uncertainty of 2 sec in t causes an uncertainty of 0.0015 in z; an uncertainty of 1 min in the half-life of Xe^{138} causes an uncertainty of 0.001 in z. The selected value from the gas sweeping experiments is 0.046 ± 0.004. This, averaged with the value from the emanation experiments (Table I), gives 0.044 ± 0.003 for the best value of z.[12]

[h] Equation (2) was used in the calculations, and the results were checked with Eq. (1). Data for one experiment are: $T = 15$ sec, $t = 40$ sec, $Q = 0.0323$, $x = 0.82 \pm 0.02$[8] giving $z = 0.0125$. Uncertainties of 2 sec in t, 0.02 in x, 10% in the half-life of Xe^{139}, and 3% in the half-life of Cs^{139} cause approximate uncertainties in z of 0.0015, 0.0008, 0.0013, and 0.0008, respectively. The error due to coprecipitation of Cs^{139} is <0.0005. Escape of Xe^{139} from solution caused z to be low by <0.002.[10]

[i] Equation (2) was used in the calculations, and the results were checked with Eq. (1). Data for one run are: $T = 15$ sec, $t = 40$ sec, $Q = 0.350$, $x = 0.59 \pm 0.01$[8] giving $z = 0.081$. Uncertainties of 2 sec in t, 0.01 in x, 10% in the half-life of Xe^{140}, and 5% in the half-life of Cs^{140} cause approximate uncertainties in z of 0.016, 0.002, 0.010, and 0.016, respectively.[10]

[j] From the intercept in Fig. 1, $H = 0.753 \pm 0.068$. A 2-sec uncertainty in τ increases the error to ± 0.080. Use of equation 3b with $x = 0.205$ $(_{-0.004}^{+0.019})$,[21] $\lambda_A = 0.23$ sec^{-1} (33% error estimated), and $\lambda_B = 0.028$

the fractional cumulative yield of the inert gas, based on the cumulative yield of the product determined, is given by

$$w = \frac{G}{E(\epsilon + G)(1 - f)}. \qquad (6)$$

The emanating power is estimated from Eq. (7)

$$E = \exp(-\lambda \delta), \qquad (7)$$

in which λ is the decay constant of the inert gas, and δ is the effective time spent by the inert gas in the stearate salt. For barium stearate[8] and lanthanum stearate $E > 0.99$ for 3.9-sec Rn^{219}, so $\delta < 0.056$ sec.

It was determined that the 3.0-sec Kr^{92} escaped from uranyl stearate as efficiently as it did from barium stearate. The fractional cumulative yield of Kr^{92}, uncorrected for emanating power, is 0.312 ± 0.005 from uranyl stearate experiments (see Table I) and 0.31 ± 0.01 from barium stearate experiments.[8] The emanating power of barium stearate for Kr^{92} is estimated from Eq. (7) to be >0.987. Therefore, from Eq. (6) the emanating power of uranyl stearate for Kr^{92} is

$$E_U = (>0.987)\frac{0.312 \pm 0.005}{0.31 \pm 0.01} = >0.95.$$

The effective time spent in uranyl stearate by Kr (and assumed to be the same for Xe) is <0.22 sec.

Half-lives have been taken from the compilation of Katcoff,[1] unless otherwise noted. Half-lives of Ba^{142}, La^{141}, and La^{142} have been taken from the paper of Schuman, Turk, and Heath.[27]

Errors given are standard deviations of averages, unless otherwise noted.

± 0.003 sec^{-1} (see Fig. 1 and the Appendix) gives the independent yield of Ba^{141} shown.[13]

[k] Equation (1) was used in the calculations. Data for one experiment are: $T = 9$ sec, $t = 21.6$ sec, $t' = 29.0$ min, $\Delta t = 29.0$ min, $Q = 0.0186$, $R = 0.00214$, $y = 0.27$ giving $z = 0.0040$. Uncertainties of 2 sec in t, 0.5 min in t', 0.08 in y, 1 min in the half-life of Ba^{141}, and 3 sec in the half-life of Cs^{141} cause approximate uncertainties in z of 0.0009, 0.0001, 0.0010, 0.0001, and 0.0004, respectively.[13]

[l] Equation (1) was used in the calculations. Data for one experiment are the same as in footnote k, except that $Q = 0.0492$ and y is unknown. For the calculations, y was assumed to be 0.5, and the half-life of Cs^{142} was taken to be 5 sec[34] giving $z = 0.020$. Values of $y = 0$ or $y = 1$ cause a variation in z of about 0.0038. Uncertainties of 2 sec in t, 0.5 min in t', 6 min in the half-life of La^{142}, 1 min in he half-life of Ba^{142}, and 3 sec in the half-life of Cs^{142} cause approximate uncertainties in z of 0.0021, 0.0003, 0.0003, 0.0011, and 0.0017, respectively.[13]

[m] Equation (1) was used in the calculations. Data for one experiment are: $T = 7.2$ sec, $t = 38.4$ sec, $t' = 102$ min, $\Delta t = 102$ min, $Q = 0.0391$, $R = 0.0107$. The value of y is unknown, and the value assumed for the calculations affects the value of z. If $y = 0$, $z = 0.009$, an upper limit for z. If $z = 0$, $y = 0.63$, an upper limit for y. On the assumption that $y = 0.2$, $z = 0.0060$. Values of $y = 0.1$ or $y = 0.3$ cause a variation in z of 0.0014. (The value of y from the Gaussian charge distribution curve for $A = 143$ is 0.17—see Discussion.) Uncertainties of 2 sec in t, 0.5 min in t' and Δt, 10% in R, 1.2 sec in the half-life of Ba^{143}, and 0.5 min in the half-life of La^{143} (taken to be 14.0 ± 0.5 min[34]) cause approximate uncertainties in z of 0.0016, 0.0003, 0.0010, 0.0010, and 0.0010, respectively.[13]

[n] Less than 1 count/min of 12.9-day Cs^{136} was found in the stearate fraction from emanation experiments. The limit on the Cs^{136} yield is $<0.045\%$, which is consistent with Nervik's[35] value of 0.035%. The fractional independent yield was estimated using 4.4% for the total yield of the 136 chain.[35]

[27] R. P. Schuman, E. H. Turk, and R. L. Heath, Phys. Rev. 115, 185 (1959).

RESULTS

The results of new measurements of fractional cumulative yields and fractional independent yields are summarized in Tables I and II. Methods of treatment of the experimental data are summarized in the footnotes to the tables. Additional information is given in the theses to which references are made. The footnotes also contain references to sources of data used in the calculations and to other measured values of the yields.[1,8,21,28–35]

DISCUSSION

Charge Distribution Curves

For thermal-neutron fission of U^{235}, the data presented in this paper together with other data[8,21,36] give fractional yield values for two or more members of the decay chains with $A = 91, 139, 140, 141, 142$, and 143. These values are plotted against Z in Fig. 2. Also shown are charge distribution curves drawn to fit the yields as well as possible without restrictions on Z_P, the position on the Z axis of the maximum in a curve. As can be seen, the curve proposed by Glendenin, Coryell, and Edwards (GCE),[2,4] which has been widely used,[4–9,36] is too broad in Z for $A = 140, 141, 142$, and 143. The data are better represented by Gaussian curves

$$P(Z) = (c\pi)^{-\frac{1}{2}} \exp[-(Z-Z_P)^2/c], \qquad (8)$$

in which $P(Z)$ is the fractional independent yield of the fission product with atomic number Z, and c is a constant for a given chain. The best single value of c for the six mass numbers is about 0.9, but the values of c for the preferred curves deviate from this value by at least ± 0.1. Summation of $P(Z)$ at unit intervals of charge gives a value close to unity, but not precisely unity as it should.

A Gaussian distribution may also be represented in cumulative form. Terrell[37] used this form for representation of the distribution of the number of neutrons emitted in fission, and we shall use it in the remainder of this paper for representation of charge distribution. This representation gives precisely unity for the sum of fractional independent yields (area under the curve).

[28] C. R. Dillard, R. M. Adams, H. Finston, and A. Turkevich, *Radiochemical Studies: The Fission Products*, edited by C. D. Coryell and N. Sugarman (McGraw-Hill Book Company, Inc., New York, 1951), National Nuclear Energy Series, Plutonium Project Record, Vol. 9, Div. IV, pp. 616 and 624.

[29] A. G. W. Cameron, Atomic Energy of Canada Limited Report AECL-433, 1957 (unpublished).

[30] B. V. Erschler and F. S. Lapteva, Atomnaya Energ. **1**, 63 (1956) [translation: Soviet J. Atomic Energy **4**, 471 (1957)].

[31] I. F. Croall, J. Inorg. & Nuclear Chem. **16**, 358 (1961).

[32] A. P. Baerg, R. M. Bartholomew, and R. H. Betts, Can. J. Chem. **38**, 2147 (1960).

[33] K. F. Flynn, from compilation by I. F. Croall, Atomic Energy Research Establishment Report AERE-R-3209, 1960 (unpublished).

[34] K. Fritze and T. J. Kennett (private communications, 1960 and 1961).

[35] W. E. Nervik, Phys. Rev. **119**, 1685 (1960).

[36] W. E. Grummitt and G. M. Milton, J. Inorg. & Nuclear Chem. **5**, 99 (1957).

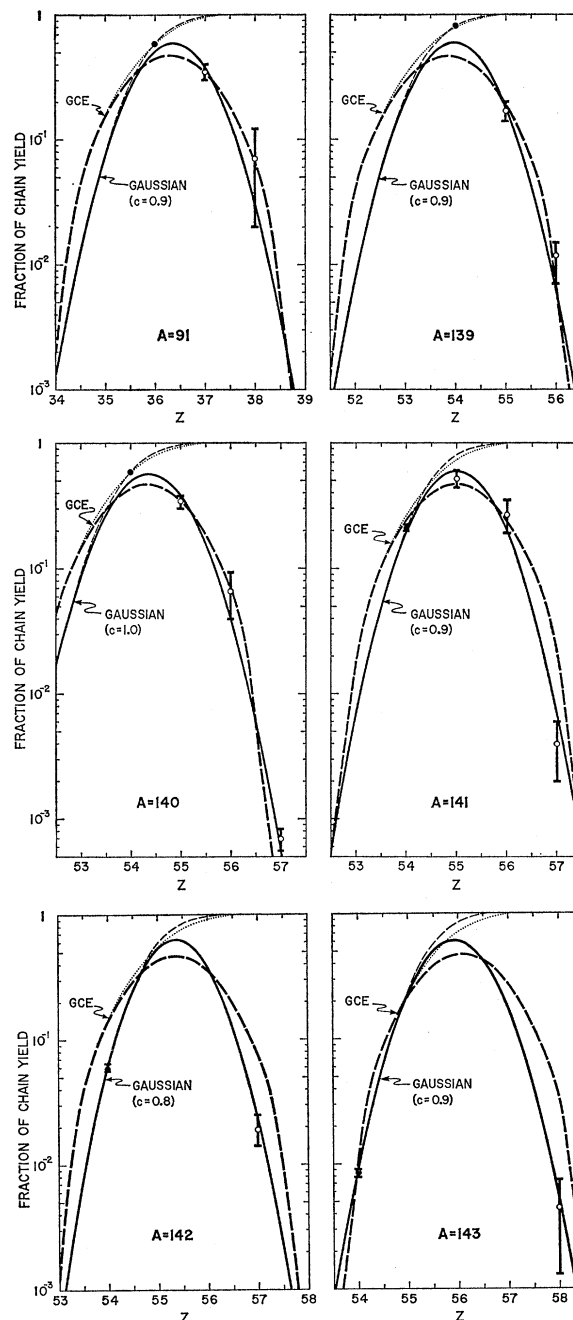[37] J. Terrell, Phys. Rev. **108**, 783 (1957).

FIG. 2. Charge distribution curves fitted to fractional-yield data: $\bigcirc$, independent yield; $\bullet$, cumulative yield. The GCE curves are those proposed by Glendenin, Coryell, and Edwards: —— for independent yields, $\cdots\cdots$ for cumulative yields. The Gaussian curves represent Eq. (8): —— for independent yields, – – – – for cumulative yields.

The fractional cumulative yield of a fission product with charge Z is given by:

$$\sum_0^Z (P_n) = \frac{1}{\sigma(2\pi)^{\frac{1}{2}}} \int_{-\infty}^{(Z+\frac{1}{2})} \exp\left[\frac{-(n-Z_P)^2}{2\sigma^2}\right] dn$$

$$= \tfrac{1}{2} + \tfrac{1}{2} f[(Z-Z_P+\tfrac{1}{2})/\sigma], \qquad (9)$$

TABLE III. Charge distribution curves.

Fission product	Fractional cumulative yield[a]	Z_P	σ
Kr^{91}	0.59 ± 0.01^b	36.32 ± 0.09	0.81 ± 0.27
Rb^{91}	0.93 ± 0.05		
Xe^{139}	0.82 ± 0.02^b	$53.82^{+0.14}_{-0.10}$	$0.75^{+0.14}_{-0.10}$
Cs^{139}	$0.988^{+0.003}_{-0.005}$		
Xe^{140}	0.59 ± 0.01^b	54.34 ± 0.03	0.68 ± 0.03
Cs^{140}	0.934 ± 0.026		
Ba^{140}	0.9993 ± 0.0001^c		
Xe^{141}	$0.205^{+0.019\,d}_{-0.004}$	54.97 ± 0.004	0.59 ± 0.03
Cs^{141}	0.726 ± 0.082		
Ba^{141}	0.9964 ± 0.0017		
Xe^{142}	$0.059^{+0.006\,d}_{-0.003}$	55.36 ± 0.04	0.55 ± 0.03
Ba^{142}	0.981 ± 0.005		
Xe^{143}	0.0085 ± 0.0005^b	$55.92^{+0.08}_{-0.10}$	0.60 ± 0.04
La^{143}	0.9956 ± 0.0030		
		Average:	0.62 ± 0.06^e

a It is assumed that independent yields are negligible for late chain members, those with $Z\geq 2$ more than the Z of the last member listed.
b From reference 8.
c From reference 36.
d From reference 21.
e The average value was obtained by weighting each individual value according to the reciprocal of the square of its estimated uncertainty.

in which $f[X]$ is a normal probability integral, tabulated in various publications[38] and given by the expression
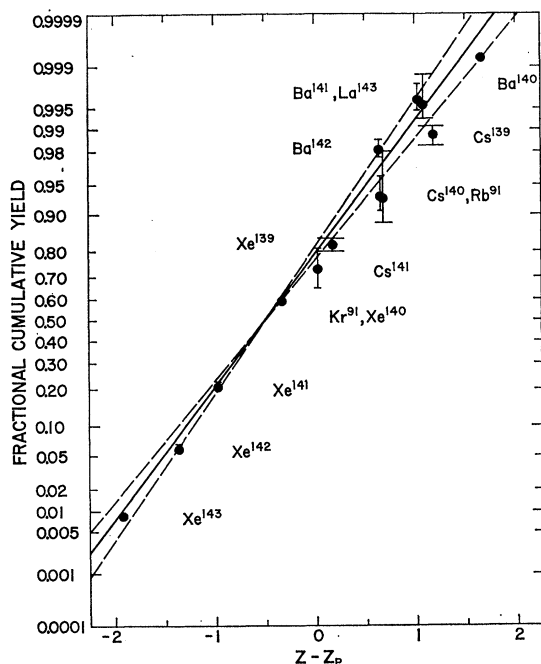

FIG. 3. Probability-scale plot of the data in Table III. The line is the Gaussian distribution curve, Eq. (9), with $\sigma=0.62\pm0.06$.

38 See, for example, Tables of Normal Probability Functions, National Bureau of Standards, Applied Mathematics Series No. 23 (Superintendent of Documents, U. S. Government Printing Office, Washington, D. C., 1953).

$$f[X]= (2\pi)^{-\frac{1}{2}}\int_{-X}^{X} \exp\left[\frac{-\alpha^2}{2}\right]d\alpha. \qquad (10)$$

It is convenient to plot fractional cumulative yield values for a given mass number as ordinate on a "probability scale" against Z as abscissa on a linear scale. If the distribution is Gaussian, the points fall on a straight line which intercepts probability 0.5 at $Z_P-0.5$ and has a slope related to the value of σ (e.g., the probability changes from 0.5 to 0.8413 over a charge range equal to the value of σ). Plots of this type were made for the six chains under discussion, and the results are summarized in Table III.

As can be seen, there is some variation in the standard deviations of the curves. However, a curve with $\sigma=0.62 \pm0.06$ is consistent with all of the data as is shown in Fig. 3. The cumulative yields listed in Table III are plotted as ordinate on a "probability scale" against $Z-Z_P$, the Z_P values being those determined from the probability plots vs Z for individual chains and listed in Table III.

The ±0.06 uncertainty in the average value of σ leads to considerable uncertainty in the relationship between $Z-Z_P$ and a low fractional cumulative or independent yield. This is appropriate because there appears to be a real spread in the widths of the curves, and a low yield value, being far removed from the curve maximum, should define it or be defined by it only poorly.

The constants c and σ in the two treatments that have been discussed are related approximately through Sheppard's correction.[39]

$$c\approx 2(\sigma^2+\tfrac{1}{12}). \qquad (11)$$

For $\sigma=0.62\pm0.06$, the corresponding value of $c\approx0.94 \pm0.15$.

The Z_P Function

The Z_P values for the six fission-product chains listed in Table III are known quite well empirically. Values for other chains, for which fractional yields of only single members are known (see Appendix, Table V), may be estimated on the assumption that the charge distribution curve defined by Eq. (9) with $\sigma=0.62\pm0.06$ is applicable. Uncertainties in experimental yields, and in σ are reflected as uncertainties in the empirical Z_P values. Of course, errors may be larger if the assumed charge distribution curve is not applicable, and it should be remembered that the curve is derived from data for only a few mass numbers with high fission yields. Curves for mass numbers with low yields might well be different in width or lack symmetry, and yields of fission products or fragments whose compositions are close to nuclear shell edges might well deviate in yield from a smooth

39 See, for example, R. A. Fisher, Statistical Methods for Research Workers (Hafner Publishing Company Inc., New York, 1958), p. 76.

curve. Suggestions have been made[3,4,8] that such yields may be abnormal.

For the purposes of analysis and illustration (Table V and Figs. 4, 5, 6, 7, and 8) empirical Z_P values are classified as follows:

A. (filled points)—Derived from the fit of an arbitrary Gaussian curve to two or more fractional-yield values (Table III).

B. (shaded points)—Derived from the fit of the assumed Gaussian curve ($\sigma = 0.62 \pm 0.06$) to the fractional yield of one fission product with a composition not close to or complementary to a major nuclear shell edge.

C. (open points)—Similar to B, except the fission product has a composition that is close to or complementary to a major nuclear shell edge (within ± 1 charge or mass unit).

I.—Derived from the fractional yield of only one of two known isomers. (Arrow to the point shows the direction the point would be shifted by addition of the fractional yield of the other isomer.)

Limit.—Derived from the upper limit on a fractional yield. (Arrow is away from the point, which is located at the position of the limit.)

Figure 4 shows a plot of the empirical Z_P values vs A, the mass number of the products after neutron evaporation from thermal-neutron fission of U^{235}. (The values of Z_P are listed in the Appendix, Table V.) The line in Fig. 4 is the Z_P function for unchanged charge distribution (UCD), calculated on the assumption that each fragment, on the average, evaporates 1.25 neutrons, half the average number, ν, of neutrons emitted in fission. As can be seen and as has been recognized since the earliest analysis[2] of charge distribution, the light fission products are richer in protons and the heavy products are poorer in protons than is U^{235} minus 2.5 neutrons. From comparison of the plot of empirical Z_P values with the yield-mass curve[1] shown above, it may be seen that there is no experimental information about charge distribution for mass numbers in the valley between the yield peaks.

For a more careful analysis of the Z_P function, it is useful to consider Fig. 5, in which both the mass and charge scales are larger than in Fig. 4. The mass scale is folded to superimpose mass numbers (A') of complementary light and heavy primary fragments, before neutron evaporation. For the ordinate a multiple of the mass number is subtracted from Z_P. The multiple chosen is (Z_F/A_F), the ratio of atomic- to mass-number for the fissioning nucleus, U^{236}; if no redistribution of charge occurred during fission, Z_P values would fall on a line with zero ordinate (UCD).

The fragment mass-number A' is estimated by increasing the product mass-number A by the average number (ν_l or ν_h) of neutrons emitted by the fragment.

$$A'_l = A_l + \nu_l,$$
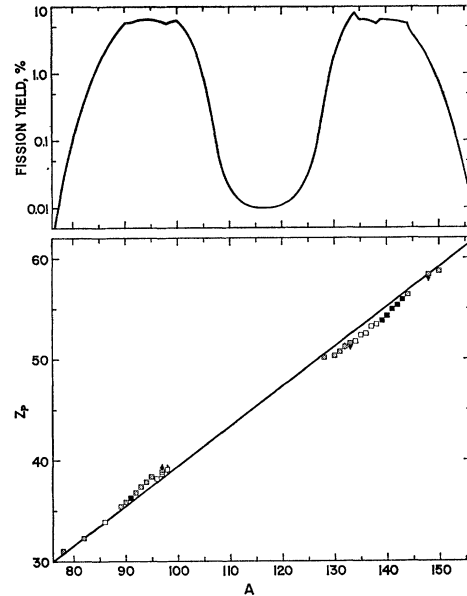$$A'_h = A_h + \nu_h. \tag{12}$$

FIG. 4. $U^{235}(n_{th}, F)$—Top: Yield-mass curve (see footnote 1). Bottom: Squares are empirical Z_P values. Line is the Z_P function for unchanged charge distribution.

The number of neutrons emitted by a fragment is estimated from Eq. (13),

$$\nu_h = 0.531\nu + 0.062(A_h - 143),$$
$$\nu_l = 0.531\nu + 0.062(A_l + 143 - A_F), \tag{13}$$

a discontinuous function constructed to represent in a simple way the composite data for the average number of neutrons emitted per fragment for $U^{235}(n_{th}, F)$,[40] $Cf^{252}(SF)$,[41] and $U^{233}(n_{th}, F)$,[42] as corrected by Terrell.[43]

In addition to the Z_P function for unchanged charge distribution, Fig. 5 shows Z_P functions for the Pappas[4] version of the equal-charge-displacement postulate (ECD)[2] and for the minimum potential energy (MPE) proposal of Swiatecki[44] as calculated by Coryell, Kaplan, and Fink[9] using Cameron's table of atomic masses.[29] As can be seen, these Z_P functions represent the empirical Z_P values poorly. Also, Coryell, Kaplan, and Fink[9] report that these and several other Z_P functions represent poorly the empirical Z_P values which they estimate using the Glendenin-Coryell-Edwards charge distribution curve.

Figure 6 shows a new empirical Z_P function drawn to be smooth and continuous and to fit the empirical values as well as possible, class A and B values (see above) being given the greatest weight. In the mass

[40] V. F. Apalin, Yu. P. Dobrynin, V. P. Zakharova, I. E. Kutikov, and L. A. Mikaelyan, Atomnaya Energ. 8, 15 (1960) [translation: Soviet J. Atomic Energy 8, 10 (1961)].
[41] S. L. Whetstone, Jr., Phys. Rev. 114, 581 (1959).
[42] J. S. Fraser and J. C. D. Milton, Phys. Rev. 93, 818 (1954).
[43] J. Terrell, Bull. Am. Phys. Soc. 6, 16(T) (1961).
[44] W. Swiatecki (private communication to C. D. Coryell).[9]

region $A' = 140$ to 145, where the empirical values are best known, there appears to be a definite rise in the ordinate of the function. This rise occurs about mid-way between the 50- and 82-neutron shell edges. The other apparent feature of the new Z_P function is its sharp rise near the 50-proton shell edge. This feature was discussed by Kennett and Thode[6] and was shown in the 1958 empirical Z_P function.[8] The sharp rise is based on the small independent yield of I^{128} and on the assumption that the assumed charge distribution curve is applicable to fission products with $A = 128$, 130, and 131.

Although the evidence for the sharp rise in Z_P near the 50-proton shell edge is admittedly weak, the inference which may be drawn from it—that fission preferentially gives isotopes of $_{50}Sn$, rather than isotopes of lower Z elements ($_{49}In$, $_{48}Cd$, $\cdots$)—may also be drawn from other experimental observations of fission.

It is well known[1] that fission yields of isotopes of elements with Z just less than 50 are small and determine the depth of the valley between the peaks in the yield-mass curve (Fig. 4). The rise in yield with increasing mass number from the valley to the heavy mass peak occurs in the mass region where yields of $_{50}Sn$ and $_{51}Sb$ nuclides establish the location of the curve.[1] The location on the A axis of the light side of the heavy mass peak is essentially the same for all low-energy fission processes that have been studied.[1,35] A preference in fission for isotopes of $_{50}Sn$ over those of lower Z elements is also suggested by these observations.

Another pertinent observation is the leveling off and decrease in total fragment kinetic energy as the fragment mass ratio approaches unity.[45-49] Over most of the
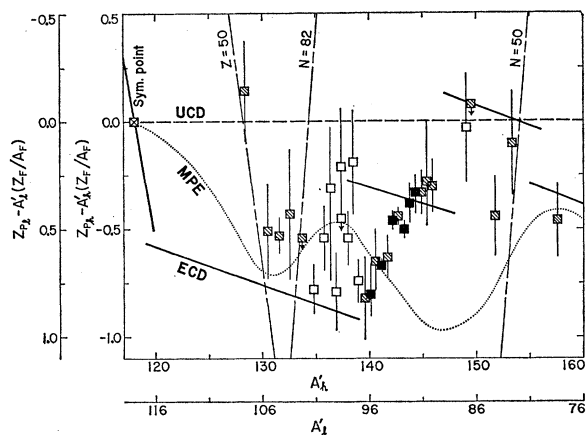

FIG. 5. $U^{235}(n_{th},F)$empirical Z_P values and some proposed Z_P functions, unchanged charge distribution (UCD), equal charge displacement (ECD), and minimum potential energy (MPE). Subscripts F, l, and h refer to the fissioning nucleus, light fragments, and heavy fragments, respectively, and A' denotes mass number before neutron emission.

[45] W. E. Stein, Phys. Rev. **108**, 94 (1957).
[46] W. E. Stein and S. L. Whetstone, Jr., Phys. Rev. **110**, 476 (1958).
[47] J. C. D. Milton and J. S. Fraser, Phys. Rev. **111**, 877 (1958).
[48] J. B. Niday, Phys. Rev. **121**, 1471 (1961).
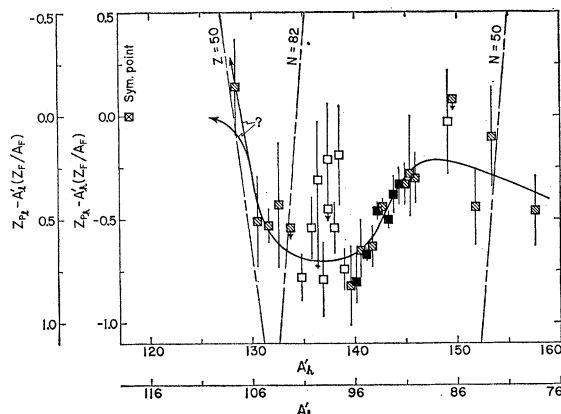[49] J. C. D. Milton and J. S. Fraser, Phys. Rev. Letters **7**, 67 (1961).

FIG. 6. Empirical Z_P function drawn to fit empirical Z_P values for $U^{235}(n_{th},F)$.

range in going from large to small mass ratios the kinetic energy increases in the way expected for essentially constant distance of fragment separation at the moment of scission and decreasing fragment charge ratios.[50] The kinetic energy appears to be derived almost entirely from the Coulomb energy between the fragments at the moment of scission.[50] The unexpected leveling off and decrease in kinetic energy can be explained as follows: The leveling off would occur if both separation distance and charge ratio remained essentially constant with changing mass ratio. (For example, the charge ratio might remain constant at 50:42 for uranium fission.) A decrease in kinetic energy in going to very small mass ratios could be caused by a decrease in the Q of the primary fission reaction, Q being the sum of the kinetic and excitation energies of the primary fragments and also the difference between the mass of the fissioning nucleus and the ground-state masses of the primary fragments. Since there is little change with mass ratio in the sum of the excitation energies of the primary fragments, as measured by the number of neutrons evaporated,[40-43] a decrease in Coulomb energy would result from a decrease in Q. Q would decrease at very small mass ratios (because of the parabolic shape of binding energy curves) if the composition of one fragment (e.g., $_{50}Sn$) were very close to the region of beta stability (Z_A) so that the composition of the complimentary fragment were very far from Z_A.[51] This view is supported by the observation[48,52] of small ranges for independently formed Rb^{86} and Cs^{136}, which, having charges close to Z_A, are complimentary to fragments with charges very far from Z_A.

A preference in fission for $_{50}Sn$ isotopes over lower-Z nuclides can be rationalized using the Vladirmirskii-Whetstone model[41,53] by assigning 50 protons and about

[50] I. Halpern, Ann. Rev. Nuclear Sci. **9**, 290 (1959).
[51] R. B. Leachman (private communication), 1960.
[52] F. Brown and B. H. Oliver, Can. J. Chem. **39**, 616 (1961).
[53] V. V. Vladimirskii, J. Exptl. Theoret. Phys. (U.S.S.R.) **32**, 822 (1957) [translation: Soviet Phys.—JETP **5**, 673 (1957)].

82 neutrons to the heavy end of the "dumbbell-shaped" distorted nucleus. A break in the neck at its juncture with the heavy end would then result in tin isotopes with low excitation energies. Neutron emission probabilities would be low, as observed[40-43] for the lightest heavy fragments and as rationalized by Whetstone.[41] The complementary fragments ($_{42}$Mo for $_{92}$U fission) would be highly excited from the deformation energy of the neck and would evaporate many neutrons,[41] as observed for the heaviest light fragments. The resulting products would undergo successive beta decays, forming fission products whose yields determine the location of the heavy side of the light mass peak and the valley in the yield-mass curve. Thus, fission products with mass numbers about one-half that of the fissioning nucleus may be formed predominantly by beta decay starting with fission products complementary to tin, not directly by symmetric fission as has been assumed.

Direct evidence against this model would be observation of independent formation of fission products with atomic numbers about one-half that of the fissioning nucleus. None has been reported for low-energy fission. Between $_{50}$Sn and its complement, only Tc^{98} from U^{235}(n_{th},F) has been reported to be formed independently (3×10^{-8} of the chain yield).[54]

For low-energy fission processes other than thermal-neutron fission of U^{235} there are insufficient published data for determination either of the charge distribution curves or of the Z_P functions. Therefore, to have something for comparison with the data that are available, we assume that the curve and function derived for thermal-neutron fission of U^{235} are applicable. Because of the sharp rise in the Z_P function near the 50-proton shell edge, we adjust the A' axis to make the abscissa point $A'_h = 50(A_F/Z_F)$ common to all fission processes. Figure 7 shows the Z_P function and empirical Z_P values, plotted as points, that are obtained from measured
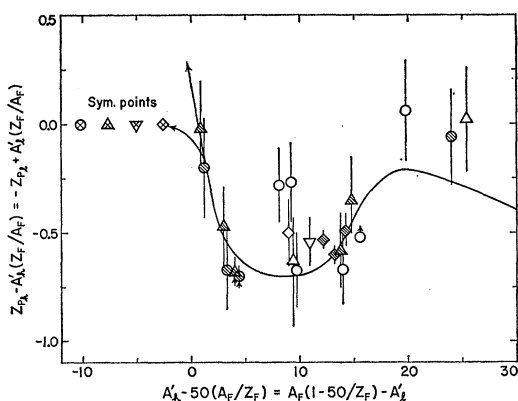

FIG. 7. Empirical Z_P function and values for: U^{233}(n_{th},F), ◯; Pu^{239}(n_{th},F), △; Cm^{242}(SF), ▽; and Cf^{252}(SF), ◇.

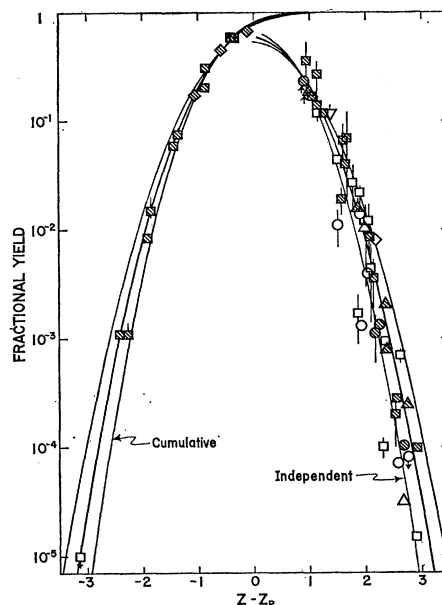[54] G. D. O'Kelley and Q. V. Larson, Abstracts, American Chemical Society Meeting, Memphis, 1955.

FIG. 8. Conventional charge distribution plot. Designation of points is the same as in Figs. 6 and 7. The curves are calculated from Eq. (9) with $\sigma = 0.62 \pm 0.06$. Z_P values are from the empirical Z_P curves shown in Figs. 6 and 7 and are listed in next to the last column of Table V.

fractional yields and the assumed charge-distribution curve. The empirical Z_P values and the coordinates of the Z_P function are listed in the Appendix, Table V.

Figure 8 shows a conventional plot of fractional chain yield vs $Z - Z_P$ for products of low-energy fission. Z_P values are from the new empirical Z_P function shown in Figs. 6 and 7.

The combination of the Gaussian charge distribution curve and the new empirical Z_P function fit most of the fractional yield data quite well. The major discrepancies are listed in Table IV. The uncertainties in the calculated values reflect the uncertainty in the charge distribution curve ($\sigma = 0.62 \pm 0.06$) and an assumed uncertainty in Z_P of ± 0.1 charge unit. Table IV shows clearly the large uncertainty in calculated values for small fractional yields.

The only discrepancies that are appreciably outside the indicated uncertainties are for the yields of Nb^{96} and Nb^{97} from thermal-neutron fission of U^{235} and U^{233} and for the yields of Xe^{136} from thermal-neutron fission of U^{235}, U^{233}, and Pu^{239}. The experimental yields of Xe^{136} are based on the mass assignment of the 83-sec iodine fission product to I^{136}, and this assignment is uncertain.[55] If the mass assignment is correct, the large yield of Xe^{136} may be associated with its neutron number of 82. The measured yield of Cs^{137}, another 82-neutron fission product, is also somewhat larger than calculated.

[55] N. R. Johnson and G. D. O'Kelley, Phys. Rev. 114, 279 (1959).

TABLE IV. Major discrepancies between calculated and measured fractional independent yields.

Fission process	Fission product	Experimental yield[a]	Calculated yield	$\dfrac{\text{(Calc. yield)}}{\text{(Expt. yield)}}$
$U^{235}(n_{th},F)$	Nb^{96}	$(1.0\pm0.2)\times10^{-4}$	$(1.8_{-1.4}^{+2.5})\times10^{-3}$	18 (4 to 45)
	Nb^{97}	$(1.7\pm0.8)\times10^{-3}$	$(1.4_{-0.8}^{+1.1})\times10^{-2}$	8 (2 to 16)
	Tc^{98}	$(3\pm2)\times10^{-8}$	$(9_{-9}^{+19})\times10^{-7}$	30 (0 to 100)
	Xe^{136}	0.52 ± 0.08 (?)	0.09 ± 0.04	0.17 ± 0.08
	Cs^{137}	$(2.2\pm0.3)\times10^{-2}$	$(1.2_{-0.9}^{+1.0})\times10^{-2}$	0.55 (0.2 to 1.0)
$U^{233}(n_{th},F)$	Nb^{96}	$(1.3\pm0.2)\times10^{-3}$	$(1.0_{-0.6}^{+0.9})\times10^{-2}$	8 (3 to 15)
	Nb^{97}	$(1.1\pm0.4)\times10^{-2}$	$(5.3_{-2.3}^{+2.6})\times10^{-2}$	5 (2 to 7)
	Rb^{86}	7×10^{-5}	$(3.8_{-3.3}^{+8.0})\times10^{-4}$	5 (1 to 17)
	Xe^{136}	0.73 ± 0.05 (?)	0.26 ± 0.05	0.36 ± 0.07
$Pu^{239}(n_{th},F)$	Rb^{86}	3.1×10^{-5}	$(2.2_{-1.9}^{+9.5})\times10^{-4}$	7 (1 to 40)
	Xe^{136}	0.68 ± 0.06 (?)	0.20 ± 0.05	0.30 ± 0.08
$Cf^{252}(SF)$	Cs^{136}	8×10^{-3}	$(3.3_{-2.3}^{+3.7})\times10^{-3}$	2.4 (1 to 8)
	Xe^{139}	0.67 ± 0.01	0.74 ± 0.06	(cumulative yield)

[a] From Appendix, Table V. Fractional independent yields for Xe^{136} and Cs^{137} are the differences between unity and the fractional cumulative yield of I^{136} or of Xe^{137}, respectively.

In fission of $_{92}U$ isotopes, $_{41}Nb$ products are complementary to $_{51}Sb$ products, and it has been proposed[8] that 51–41 (and 49–43) proton splits may be low in yield because of competition from favored 50–42 splits. In addition, part of the independent yield of Nb^{96} may lead to an undetected isomer.[8] It is interesting, and perhaps significant, that the measured yields of Nb^{96} and Nb^{97} from thermal-neutron fission of Pu^{239} are close to the calculated values. Here, $_{41}Nb$ products are complementary to $_{53}I$ products, which are three protons removed from the 50-proton shell edge.

Wolfsberg's[56] preliminary results for the fractional cumulative yields of krypton and xenon isotopes from thermal-neutron fission of U^{233} and Pu^{239} are represented quite well by the charge-distribution formulation just discussed, except that for Pu^{239} fission the measured Kr yields are lower than predicted.

In conclusion, we wish to make clear that although our treatment of nuclear-charge distribution is reasonably consistent with available experimental data, it is little more than an empirical correlation. Only for thermal-neutron fission products of U^{235} in the mass regions near $A=141$ and at $A=91$, where the charge distribution curves have been studied, do we have some true knowledge of charge dispersion. Elsewhere, information is restricted to one fractional yield per chain, and there are two unknowns, Z_P and the charge distribution curve. Assumption of knowledge of one fixes the other, and perhaps creates a self-consistent and

reasonable picture. This does not, however, constitute true knowledge of nuclear-charge distribution.

---

[56] K. Wolfsberg (private communication, 1961).

APPENDIX

TABLE V. Empirical Z_P values.[a]

Fission product	Fractional chain yield, independent, *cumulative	Z_P (empirical)	A'	$Z_P - A'(Z_F/A_F)$ (empirical)	$A'_h - 50$ $\times (A_F/Z_F)$	$Z_P - A'(Z_F/A_F)$ (curve)	Z_P (curve)	Class
$U^{235}(n_{th},F)$:								
As^{78}	$(8.5\pm2.5)\times10^{-3}$ [b]	31.02 ± 0.17	78.4	0.46	29.3	0.38	30.94	B
$A=79$			79.5		28.2	0.35	31.34	
$A=80$			80.5		27.2	0.33	31.71	
$A=81$			81.6		26.1	0.31	32.12	
Br^{82}	$(2\pm1)\times10^{-4}$	32.30 ± 0.24	82.6	0.10	25.1	0.29	32.49	B
$A=83$			83.7		24.0	0.27	32.90	
$A=84$			84.8		22.9	0.25	33.31	
$A=85$			85.8		21.9	0.23	33.68	
Rb^{86}	1.5×10^{-5} [c]	33.91 ± 0.25	86.9	0.03	20.8	0.22	34.10	C
$A=87$			88.0		19.7	0.21	34.52	
$A=88$			89.0		18.7	0.22	34.91	
Kr^{89}	*0.960 ± 0.004	35.42 ± 0.12	90.1	0.30	17.6	0.25	35.37	B
Kr^{90}	*0.86 ± 0.02	35.84 ± 0.10	91.1	0.33	16.6	0.30	35.81	B
Y^{90}	$<8\times10^{-5}$ [d]	<36.38	91.1	<0.87	16.6	0.30	35.81	B[e]
$A=91$	(from Table II)	36.32 ± 0.09	92.2	0.38	15.5	0.39	36.33	A
Kr^{92}	*0.31 ± 0.01	36.81 ± 0.04	93.3	0.44	14.3	0.50	36.87	B
Kr^{93}	*$0.075_{-0.002}^{+0.010}$	37.39 ± 0.10	94.3	0.63	13.4	0.59	37.35	B
Kr^{94}	*$0.015_{-0.002}^{+0.005}$	37.84 ± 0.15	95.4	0.65	12.3	0.65	37.84	B
Kr^{95}	*$(11_{-1}^{+3})\times10^{-4}$	38.40 ± 0.19	96.4	0.82	11.3	0.68	38.26	B
Nb^{96}	$(1.0\pm0.2)\times10^{-4}$	38.20 ± 0.24	97.5	0.19	10.2	0.69	38.70	C
Kr^{97}	*$<1\times10^{-5}$	>38.89	98.6	>0.45	9.1	0.70	39.14	C
Nb^{97}	$(1.7\pm0.8)\times10^{-3}$	38.65 ± 0.27	98.6	0.21	9.1	0.70	39.14	C
Tc^{98}	$(3\pm2)\times10^{-8}$	$39.14_{-0.34}^{+0.43}$	99.6	0.31	8.1	0.70	39.53	C
$A=99$			100.7		7.0	0.69	39.95	
$A=100$			101.8		5.9	0.67	40.35	
$A=101$			102.8		4.9	0.63	40.70	
Rh^{102}	$<2\times10^{-7}$	<41.66	103.9	<1.16	3.8	0.60	41.10	B[e]
$A=103$			105.0		2.7	0.49	41.42	
$A=104$			106.0		1.7	0.28	41.60	
$A=105$			107.1		0.6	0.12 or −0.02	41.87 or 41.73	
I^{128}	$(9.8\pm1.0)\times10^{-5}$ [f]	50.19 ± 0.23	128.4	0.14	0.1	0.16 or −0.08	50.21 or 49.97	B
$A=129$			129.5		1.2	−0.16 or −0.18	50.32 or 50.30	
I^{130}	$(2.8\pm0.2)\times10^{-4}$ [f]	50.36 ± 0.22	130.5	−0.51	2.2	−0.42	50.45	B
Te^{131}	0.12 [g]	50.77 ± 0.08	131.6	−0.53	3.3	−0.55	50.75	B
I^{131}	<0.01	<51.20	131.6	<-0.10	3.3	−0.55	50.75	B[e]
Te^{132}	0.36 ± 0.17	51.26 ± 0.30	132.6	−0.43	4.3	−0.62	51.07	B
I^{132}	<0.01	<51.20	132.6	<-0.49	4.3	−0.62	51.07	B[e]
I^{133}	<0.05	<51.58	133.7	<-0.54	5.4	−0.66	51.46	B
Xe^{133}	<0.001	<51.77	133.7	<-0.35	5.4	−0.66	51.46	B[e]
I^{134}	0.12 ± 0.02	51.77 ± 0.11	134.8	−0.78	6.5	−0.69	51.86	C
Xe^{135}	0.037 ± 0.012	52.40 ± 0.15	135.8	−0.54	7.5	−0.70	52.24	C
I^{136}?	*0.48 ± 0.08 [h]	53.53 ± 0.13	136.9?	0.16?	8.6	−0.70	52.67	C[e]
Cs^{136}	$(9.4\pm0.4)\times10^{-4}$ [i]	52.58 ± 0.18	136.9	−0.79	8.6	−0.70	52.67	C
Xe^{137}	*0.978 ± 0.003	53.26 ± 0.12	138.0	−0.54	9.7	−0.70	53.10	C
Xe^{138}	*0.956 ± 0.003	53.45 ± 0.10	139.0	−0.74	10.7	−0.69	53.50	C
$A=139$	(from Table III)	$53.82_{-0.10}^{+0.14}$	140.1	−0.80	11.8	−0.66	53.96	A
$A=140$	(from Table III)	54.34 ± 0.03	141.1	−0.67	12.8	−0.62	54.39	A
$A=141$	(from Table III)	54.97 ± 0.04	142.2	−0.46	13.9	−0.55	54.88	A
$A=142$	(from Table III)	55.36 ± 0.04	143.3	−0.50	15.0	−0.43	55.43	A
$A=143$	(from Table III)	$55.92_{-0.10}^{+0.08}$	144.3	−0.33	16.0	−0.35	55.90	A
Xe^{144}	*$(1.1\pm0.1)\times10^{-3}$	$56.40_{-0.20}^{+0.28}$	145.4	−0.28	17.1	−0.28	56.40	B
$A=145$			146.5		18.2	−0.23	56.88	
$A=146$			147.5		19.2	−0.21	57.29	
$A=147$			148.6		20.3	−0.21	57.72	
Pm^{148}	$<1\times10^{-4}$	<58.40	149.6	<0.08	21.3	−0.22	58.10	B
$A=149$			150.7		22.4	−0.24	58.51	
Pm^{150}	$(2.1\pm0.1)\times10^{-3}$ [j]	58.74 ± 0.18	151.8	−0.44	23.5	−0.26	58.92	B
$A=151$			152.8		24.5	−0.28	59.23	
$A=152$			153.9		25.6	−0.30	59.69	
$A=153$			155.0		26.7	−0.32	60.10	
$A=154$			156.0		27.7	−0.34	60.47	
$A=155$			157.1		28.8	−0.36	60.88	
$A=156$			158.1		29.9	−0.39	61.24	

TABLE V (continued).

Fission product	Fractional chain yield, independent, *cumulative	Z_P (empirical)	A'	$Z_P - A'(Z_F/A_F)$ (empirical)	$A'_h - 50 \times (A_F/Z_F)$	$Z_P - A'(Z_F/A_F)$ (curve)	Z_P (curve)	Class
$U^{233}(n_{th},F)$:								
Br^{82}	$(1.1\pm0.5)\times10^{-3}$ k	32.61 ± 0.22	82.8	0.06	24.0	0.27	32.82	B
Rb^{86}	7×10^{-5} c	34.14 ± 0.23	87.0	-0.06	19.8	0.21	34.41	C
Y^{90}	$<8\times10^{-5}$ d	<36.38	91.2	<0.52	15.6	0.38	36.24	C
Nb^{96}	$(1.3\pm0.2)\times10^{-3}$	38.64 ± 0.18	97.6	0.27	9.2	0.70	39.07	C
Nb^{97}	$(1.1\pm0.4)\times10^{-2}$	39.08 ± 0.17	98.7	0.28	8.1	0.70	39.50	C
I^{128}	$(1.0\pm0.1)\times10^{-4}$ f	50.20 ± 0.23	128.4	-0.20	1.2	-0.16 or -0.18	50.32 or 50.30	B
I^{130}	$(1.3\pm0.2)\times10^{-3}$ f	50.64 ± 0.18	130.5	-0.67	3.3	-0.55	50.76	B
Te^{131m}	0.23 g	51.04 ± 0.05	131.6	-0.70	4.4	-0.63	51.11	B, I
I^{136}?	$*0.27\pm0.05$ h	53.83 ± 0.08	136.9?	0.01?	9.7?	-0.70?	53.12?	C^i
Cs^{136}	$(1.4\pm0.4)\times10^{-2}$ k	53.15 ± 0.17	136.9	-0.67	9.7	-0.70	53.12	C
La^{140}	$(3.8\pm0.1)\times10^{-3}$ d	54.84 ± 0.16	141.2	-0.67	14.0	-0.54	54.97	C
$Pu^{239}(n_{th},F)$:								
Rb^{86}	3.1×10^{-5} c	34.02 ± 0.24	86.9	-0.02	25.4	0.29	34.33	C
Nb^{96}	$(7.7\pm1.0)\times10^{-4}$	38.54 ± 0.20	97.5	0.35	14.8	0.45	38.64	B
Nb^{97}	$(1.5\pm0.4)\times10^{-2}$	39.16 ± 0.17	98.5	0.58	13.8	0.56	39.14	B
I^{128}	$(2.4\pm0.2)\times10^{-4}$ f	50.35 ± 0.22	128.6	-0.02	0.9	-0.07 or -0.14	50.30 or 50.23	B
I^{130}	$(2.0\pm0.1)\times10^{-3}$ f	50.72 ± 0.18	130.7	-0.47	3.0	-0.53	50.66	B
Te^{131m}	0.18 g	50.94 ± 0.06	131.8	-0.68	4.1	-0.61	51.01	B, I
I^{136}?	$*0.32\pm0.06$ h	53.78 ± 0.10	137.1?	0.08?	9.4?	-0.70?	53.00?	C^i
Cs^{136}	$(1.0\pm0.7)\times10^{-2}$ d	$53.07_{-0.03}^{+0.20}$	137.1	-0.63	9.4	-0.70	53.00	C
$Cm^{242}(SF)$:								
Cs^{136}	0.12 ± 0.02 m	53.77 ± 0.11	136.9	-0.54	10.9	-0.68	53.63	C
$Cf^{252}(SF)$:								
Cs^{136}	0.008 n	53.01 ± 0.15	137.6	-0.50	9.0	-0.70	52.81	C
Xe^{139}	$*0.67\pm0.01$	54.23 ± 0.04	140.8	-0.53	12.2	-0.65	54.11	B
Xe^{140}	$*0.45\pm0.01$	54.58 ± 0.04	141.9	-0.60	13.3	-0.59	54.59	B
Xe^{141}	$*0.172\pm0.005$	55.08 ± 0.07	142.9	-0.49	14.3	-0.50	55.07	B
Xe^{144}	$*<0.007$	>55.62	146.1	>-1.20	17.5	-0.26	56.56	B^l

a Yields are from this paper or from the compilation in reference 8 unless another reference is given. Corrections for delayed neutron emission were considered, but none were made because those that could be applied with some degree of certainty were insignificant. Z_P values based on two or more yields are from Table III. Z_P values based on a single yield were calculated on the assumption that the charge distribution curve defined by Eq. (9) with $\sigma = 0.62\pm0.06$ was applicable. Subscript F refers to the fissioning nucleus, and A' denotes the average mass number of the fission fragments before neutron emission that give fission products with the mass number denoted in column 1. "Class" is discussed in the text.
Values of constants used are:

	ν	Z_F/A_F	$50(A_F/Z_F)$
$U^{235}(n_{th},F)$	2.5	0.3898	128.3
$U^{233}(n_{th},F)$	2.5	0.3932	127.2
$Pu^{239}(n_{th},F)$	2.9	0.3917	127.7
$Cm^{242}(SF)$	2.5	0.3967	126.0
$Cf^{252}(SF)$	3.8	0.3889	128.6

b A. Kjelberg and A. C. Pappas, J. Inorg. & Nuclear Chem. 11, 173 (1959).
c From reference 1 and W. E. Grummitt, M. Nussis, and G. Lahaie, Third Symposium on Nuclear and Radiochemistry, Chalk River, Ontario, September, 1960 (unpublished), Paper No. 16.
d From references 36 and 1.
e Not shown in Figs. 4, 5, 6 or 8.
f From references 1 and 6.
g L. E. Glendenin, E. P. Steinberg, and M. Talat-Erbem (private communication, 1960).
h From reference 1.
i From reference 32.
j Y. Y. Chu, Ph.D. thesis, University of California, Berkeley, 1959 (unpublished).
k From reference 1 and D. C. Santry and L. Yaffe, Can. J. Chem. 38, 421 (1960).
l Not shown in Figs. 7 or 8.
m E. P. Steinberg and L. E. Glendenin, Phys. Rev. 95, 431 (1954).
n From reference 35.

Half-Lives

Rb^{91}: Values of the radioactivity ratio Q for Sr^{91} were measured[10] as a function of the time interval τ after the mean time of irradiation. The results are shown in Fig. 1 plotted in accordance with Eq. (3). The errors shown are the 5% uncertainties estimated for the Q values. The line is the one fitted to the data by the method of least-squares by means of Moore's and Zeigler's procedure,[57] in which the data are weighted in proportion to the reciprocal of the square of their uncertainties. The half-life of Rb^{91} obtained from the slope of the line is (72 ± 8) sec.

No allowance has been made in the calculations for possible errors in τ. We think that most of the uncertainty in τ is systematic and would be in the same direction for a given set of data and would, therefore, affect the decay-constant value obtained from the slope very little.

Kofoed-Hansen and Nielsen[58] reported a value of 100 sec for the Rb^{91} half-life. They also reported the existence of a 14-min Rb^{91} isomer produced in fission and decaying to Sr^{91}.

We looked for the 14-min Rb^{91} by separating Sr^{91} from fission-product rubidium purified after decay of the 72-sec Rb^{91} was essentially complete. We found

57 R. H. Moore and R. K. Zeigler, Los Alamos Scientific Laboratory Report LA-2367, 1960 (unpublished).

58 O. Kofoed-Hansen and K. O. Nielsen, Kgl. Danske Videnskab. Selskab, Mat.-fys. Medd. 26, No. 7 (1951).

none, and concluded that $<5\times10^{-4}$ of the Sr^{91} produced in fission grows from a 14-min rubidium parent.

We believe that our data refute the experimental evidence for the existence of a 14-min isomeric state of Rb^{91}.

Rb^{92}: Values of the ratioactivity ratio Q for Sr^{92} were unity within experimental error for the shortest separation times that were achieved ($\tau=34$ to 38 sec). The average of four values of Q is 0.97, and the estimated experimental error is ±0.05. Use of Eq. (3) and adoption of $Q>0.92$, $\tau<38$ sec, $x=0.31\pm0.01^8$ and $z<0.2$ (estimated from the Gaussian charge distribution curve, Eq. (9) with $\sigma=0.62\pm0.06$, positioned to fit the Kr^{92} cumulative yield[8]) gives $\lambda_B>0.065$ sec^{-1}, a value corresponding to half-life of <11 sec for Rb^{92}.

Our data are consistent with the value of 5.3 ± 0.5 sec reported recently by Fritze and Kennett.[59]

Kr^{97}: As shown in Table I, $<2\times10^{-4}\%$ of fission-product Zr^{97} results from the decay of an inert gas that emanates from uranyl stearate. This is inconsistent with the report of Dillard, Adams, Finston, and Turkevich[28] that 0.15% of Zr^{97} descends from an inert gas that is swept from solution, because for all other inert-gas fission products the fraction escaping from stearate salts is greater than the fraction escaping from gas-swept solutions. (Compare data in reference 8 and Table I with data in reference 28.)

We believe that our data refute the experimental evidence for the existence of Kr^{97}.

Nb^{98}: In the beta decay of niobium samples separated from zirconium soon after irradiation, there appeared a 51-min period in addition to the 73-min period of Nb^{97}.[11] The 51-min period was identified with Nb^{98} by its formation from the (n,p) reaction on Mo^{98}.

Molybdenum (as MoO_3) enriched to 96.4% Mo^{98} was irradiated with unmoderated (<14-Mev) neutrons produced from 10-Mev deuterons incident on a beryllium target at the Washington University Cyclotron. The neutron energy was less than the calculated threshold value of about 16 Mev for the $^{98}Mo(n,d)Nb^{97}$ reaction. The ratio of the yield of the 51-min activity to the yield of the 73-min Nb^{97} divided by the ratio of Mo^{98} to Mo^{97} isotopic abundances was 0.3 ± 0.1, the same (0.32 ± 0.2) as that found for a natural molybdenum target.

The mass assignment of $A=98$ and the half-life of 51 ± 3 min reported here agree with the values determined independently by Orth and Smith[60] (half-life 51.5 ± 1.0 min).

The fission yields of the 51-min Nb^{98} from thermal-neutron fission of U^{233}, U^{235}, and Pu^{239} were determined to be $(0.20\pm0.03)\%$, $(0.064\pm0.012)\%$, and $(0.20\pm0.03)\%$, respectively.[11] These represent only $(4.0\pm0.5)\%$, $(1.1\pm0.2)\%$, and $(3.3\pm0.5)\%$ of the total chain yields; thus most of the $A=98$ chain must decay

via another Nb^{98} isomer, for which Orth and Smith[60] have set a half-life limit of <2 min.

No fission product precursor of the 51-min Nb^{98} has been observed. Niobium was separated from old fission-product zirconium, but no Nb^{98} was found. If the zirconium precursor is long lived, its half-life is greater than 10^4 years.

Cs^{141}: Values of the radioactivity ratio Q for Ba^{141} were measured[10,13] as a function of τ. The data are plotted in Fig. 1. The errors reflect the estimated uncertainties in Q, 5% for the initial determinations[10] and 3% for later determinations.[13] The line is the one fitted to the data by the method of least-squares by means of Moore's and Zeigler's procedure.[57] The half-life of Cs^{141} obtained from the slope of the line is (25 ± 3) sec.

This value is in good agreement with the value of (24 ± 2) sec determined by Fritze and Kennett.[34]

Cs^{142}: Values of the radioactivity ratio Q for Ba^{142} were determined from the same samples used for Ba^{141}, and all values were unity within experimental error. Four initial determinations[10] with $\tau=35$ to 42 sec gave an average value of Q of 0.95 with an estimated uncertainty of 5%. Three later determinations[13] with $\tau=22$ to 30 sec gave an average Q value of 1.02 with an estimated uncertainty of 3%. Use of Eq. (3) and adoption of $Q>0.97$, $\tau<30$ sec, $x=0.059_{-0.003}^{+0.006}$ [21] and $z<0.5$ [estimated from the Gaussian charge distribution curve for $A=142$ (Table III)] gives $\lambda_B>0.09$ sec^{-1}, a value corresponding to a half-life of <8 sec for Cs^{142}.

Our data are consistent with the preliminary value of about 5 sec determined by Fritze and Kennett.[34]

Ba^{143}: Values of $(1-Q)$ were measured directly for La^{143} by rapid precipitation of $La(OH)_3$ and $Ce(OH)_3$ and determination of Ce^{143} in the filtrates. La^{140} tracer was added before the precipitation to make possible a correction for the 0.7 to 1.5% of lanthanum that passed through the filter. Six values of $(1-Q)$ for $\tau=42$ to 117 sec were fitted to Eq. (3) (with $F=0$) by the least-squares procedure of Moore and Zeigler.[57] The half-life value of Ba^{143} obtained was (12.0 ± 1.2) sec. The data are plotted in Fig. 1.

The intercept at $\tau=0$ is 1.20 ± 0.32, and the quantity H has a value of 1.06 ± 0.28, after correction for errors introduced by the approximations made in the derivation of Eq. (3). There are too many unknown parameters in Eq. (3b) for evaluation of any one of them. However, the value of H is consistent with the Cs^{143} and Ba^{143} half-lives of <5 sec[34] and 12 sec, respectively, and values of $x=0.24$ and $z=0.17$ obtained from the Gaussian charge distribution curve for $A=143$ (Table III).

Rapid Separations

Krypton and Xenon: Modifications of the emanation technique of Wahl[8] were used in most experiments. The general design of the irradiation container has been described.[8] The container used in the Cf^{252} experiments

[59] K. Fritze and T. J. Kennett, Can. J. Phys. **38**, 1614 (1960).
[60] C. J. Orth and R. K. Smith, J. Inorg. & Nuclear Chem. **154**, (1960).

was modified to allow periodic evacuation during long irradiations. Many of the observations described in the following paragraphs were involved in the calculations of fractional cumulative yields.

Uranyl stearate and lanthanum stearate were prepared by mixing warm aqueous solutions of sodium stearate and uranyl nitrate or lanthanum chloride in the same manner in which Wahl and Daniels[61] prepared barium stearate. The emanating power of a preparation of lanthanum stearate containing Ac^{227} was determined by the lead-sulfide method[61] to be $>99\%$ for 3.9-sec Rn^{219}. The emanating power of uranyl stearate was determined to be $>95\%$ for 3-sec Kr^{92} (see section on calculations).

About 300 mg of uranyl stearate powder having a bulk density of 0.18 g/cc was used in each experiment with U^{235}. The true density was 2 g/cc, so most of the volume occupied by the powder was empty space, which constituted 1.4% of the total volume of the container.

It was found that 3% of the recoiling fission fragments left the uranyl stearate and entered the filter-paper shield or the aluminum dish containing the powder. No significant fraction of inert-gas atoms with half-lives <3.9 min emanated from the paper or the aluminum.

About 55 mg of lanthanum stearate or barium stearate (about 20 mg/cm^2) was used in the experiments with Cf^{252}. The stearate compound occupied about 0.5% of the total volume. It was assumed that all fission fragments stopped either in the stearate compound or in the platinum source backing and that no inert-gas atoms emanated from the platinum.

Collection of the active deposit on the filter-paper linear has been shown to be essentially complete $(98\pm3\%)$.[8]

It was found that the lanthanum stearate (and all lanthanum salts that were tested) contained a small amount of Ac^{227}. Since the decay product Ra^{223} follows barium chemistry, a small correction, determined by blank experiments, had to be made to measured counting rates of barium samples separated from lanthanum stearate.

In two experiments 17-min Xe^{138} was separated from 32-min Cs^{138} by dissolution of freshly-irradiated uranyl nitrate hexahydrate (UNH) powder in hot aqueous solutions, swept with helium. About 10 g of powder was dissolved in 40 ml of solution maintained at 95°C in a 40-mm fritted funnel, up through which and through the solution helium was rapidly passing. The powder dissolved in about 4 sec. The separation was assumed to occur 2 sec after addition of the powder to the solution. This assumption is reasonable in view of the facts that inorganic salts are very poor emanators[62] and that

[61] A. C. Wahl and W. R. Daniels, J. Inorg. & Nuclear Chem. 6, 278 (1958).

[62] See, for example, A. C. Wahl, *Radioactivity Applied to Chemistry*, edited by A. C. Wahl and N. A. Bonner (John Wiley & Sons, Inc., New York, 1951), Chap. 9, p. 284.

52-sec Rn^{220} and 3.9-sec Rn^{219} are removed efficiently from hot, gas-swept solutions.[61]

Strontium and Barium: Strontium and barium nitrates, together or separately, were precipitated from cold concentrated nitric acid. About six volumes of cold 90% HNO_3 were mixed with one volume of solution containing irradiated UO_2^{++}, and Sr^{++} and/or Ba^{++} carrier. About 10 sec after addition of the HNO_3, a portion of the suspension was drained into a fritted funnel (70 mm diameter, "M" porosity) to which suction had been applied. Immediately after the filtration, the precipitate was washed with three 10-ml portions of cold fuming HNO_3. Tracer experiments showed that only 0.1% of Rb^+ and 0.03% of Cs^+ remained with the precipitate.

The effective time of separation was taken as the mean filtration time. This was a good approximation if: (1) the rate of filtration was uniform, (2) the filtration time was much shorter than the half-life of the parent nuclide, (3) no appreciable decay of the daughter nuclide occurred during the filtration, (4) new daughter nuclide formed in solution was carried by the precipitate, and (5) essentially no parent nuclide remained with the precipitate after the filtration (before the precipitate was washed).[10] Experimental conditions were checked and found to meet the above requirements quite well. The effective separation time (taken as the mean filtration time) was estimated to be known to within 2 sec.

Since it was found that some 41-sec Xe^{139} escaped from solution before the delayed separation, the radioactivity of Ba^{139} (and of Ba^{140}) that would have been observed was calculated from the activity of an internal standard, Sr^{92}, which descends from short-lived precursors.[10,59] More than 99% of the Sr^{92} was formed before the fast separation. The Sr^{92} standard was calibrated by use of activity ratios of Ba^{139}, Ba^{140}, and Sr^{92} obtained from irradiated solid UNH that was not dissolved until essentially all of the Xe^{139} had decayed. The possible escape of xenon from solution before the fast separation caused little error; it was estimated that the escape caused the measured independent yield of Ba^{139} to be low by <0.002.[10]

Lanthanum: Lanthanum hydroxide was precipitated from warm ammonium hydroxide solution. About 8 ml of irradiated solution containing about 1 g of UO_2^{++}, 20 mg of La^{3+}, 40 mg of Ba^{++} tagged with Ba^{140} tracer, and 4 g of $NH_2OH \cdot HCl$ was added to 30 ml of warm solution containing 5 g of $NH_2OH \cdot HCl$ and 16 ml of concentrated NH_4OH. After a few seconds of stirring, a portion of the suspension was filtered, and the $La(OH)_3$ washed with $0.5M$ $NH_2OH \cdot HCl$ solution adjusted to pH 8 to 9 with NH_4OH. The amount of barium remaining with the precipitate varied from 0.05 to 0.5% and was determined in each experiment from the fraction of Ba^{140} activity remaining with the precipitate.

Cerium: Cerium(IV) iodate was precipitated from $4M$ HNO_3. About 8 ml of irradiated solution containing about 1 g of UO_2^{++}, 0.5 mg each of Ba^{++} and La^{3+} carriers, and La^{140} tracer was added to 21 ml of $9M$ HNO_3 containing 30 mg of Ce^{3+} carrier. To the resulting solution was added, first, 5 ml of warm $1M$ $NaBrO_3$ solution, which rapidly oxidized Ce(III) to Ce(IV), and then 15 ml of warm $0.35M$ HIO_3. After being stirred for about 15 sec, a portion of the mixture was filtered, and the $Ce(IO_3)_4$ washed with a solution $0.1M$ in HIO_3 and $5M$ in HNO_3. The fraction of lanthanum remaining with the precipitate varied from 0.5 to 1.5% and was determined from the fraction of La^{140} activity remaining with the precipitate.

Niobium: Barium fluorozirconate was precipitated from $3M$ HCl, $5M$ HF solution, leaving niobium in solution. Irradiated UNH or an aluminum recoil catcher was dissolved in 30 ml of $4M$ HCl containing 20 mg of Zr(IV) carrier and 100 mg of Nb(V) carrier present as the oxalate complex. The solution was divided into two approximately equal portions, and 3 ml of $30M$ HF was added to one. After the resulting solution had been stirred about 1 min, $BaCl_2$ solution was added to precipitate $BaZrF_6$. The supernatant was separated by centrifugation, and the precipitation repeated two or three more times. Tracer experiments with Zr^{97} showed that 97 to 98% of the zirconium was removed by the first precipitation, and 99.97% in a total of three precipitations. The effective separation time was taken as the mean time of the first centrifugation, which lasted 40 sec. In estimating errors, we have considered that separation of niobium from zirconium could have occurred as early as the time at which $BaZrF_6$ formed or as late as the end of centrifugation.

Nuclear Rotational Spectra, the Elliott Model, and the P_2 Force*

RAYMOND S. WILLEY

Institute of Theoretical Physics, Department of Physics, Stanford University, Stanford, California

(Received November 27, 1961)

The essential features of the Elliott model with the momentum-dependent quadrupole-quadrupole operator which leads to $L(L+1)$ rotational spectra are reviewed. The operator is reduced to a momentum-independent residual interaction which differs somewhat from the P_2 interaction. The model Hamiltonian is separated into a rotational Hamiltonian, a deformed "intrinsic" Hamiltonian, and a perturbation term. The eigenfunctions and eigenvalues of the "intrinsic" Hamiltonian are found and used in Inglis' cranking model formula to calculate the moment of inertia. The model is modified, in a simple configuration, by taking a mixture of the long-range "P_2" interaction with the short-range δ-function force. For an intermediate mixture the spectrum obtained resembles the spectrum predicted by the collective vibrational Model. Finally, the implications of a P_2 residual interaction for direct-interaction inelastic scattering processes are considered. The question is discussed whether one can actually see the P_2 residual interaction in rotational nuclei, and, if so, whether the strength of the P_2 interaction determined from such scattering experiments is consistent with the strength determined from the observed rotational spectra. Within the rough approximations made, the few experimental results available are not inconsistent with the calculation.

I. INTRODUCTION

THE purpose of this paper is to explore some consequences and modifications of the nuclear model discussed by Elliott.[1]

In the simplest version of the shell model, all nucleons move independently in a central potential which is supposed to represent the averaged effect of all interactions between the particles. We take the average central potential to be a spherical harmonic oscillator potential. We neglect the spin-orbit force and work in LS coupling:

$$H_0 = \sum_{i=1}^{\nu} H_0(i) = \sum_{i=1}^{\nu} \tfrac{1}{2}(p_i^2 + r_i^2) \qquad (1.1)$$

(in units $\hbar = \omega_0 = M = 1$). ν is the number of particles in the outermost shell. (The closed shells do not enter into the calculation and we drop them from the Hamiltonian.) In LS coupling a shell-model orbital state or configuration is specified as $l_a^{\nu_a} l_b^{\nu_b} \cdots$, where $\nu_a + \nu_b + \cdots = \nu$. The oscillator potential has the well known degeneracy of single-particle levels

$$|\, 1s \,|\, 1p \,|\, 2s \; 1d \,|\, 2p \; 1f \,|\, 3s \; 2d \; 1g \,|\, \cdots ,$$

i.e., $l = N$, $N-2$, $\cdots$, 1, or 0 where $E_N = N + \tfrac{3}{2}$. Thus, all configurations for which l_a, l_b, $\cdots$ belong to the same degenerate oscillator shell will be degenerate.

Elliott[1] has developed a coupling scheme appropriate for this situation which groups together states of angular momenta characteristic of a rotational band. He showed the similarity between the states determined by this coupling scheme and the states appearing in the

[1] J. P. Elliott, Proc. Roy. Soc. (London) A245, 128, 562 (1958).